



ORIGINAL RESEARCH OPEN ACCESS

Feasibility of Round Window Exposure via External Auditory Canal: Classification and Predictive Landmarks

Jiayu Sun^{1,2,3}  | Haoyue Tan^{1,2,3} | Jianqing Chen^{1,2,3} | Jia Guo⁴ | Chengyu Zhang⁴ | Zhaoyan Wang^{1,2,3} | Hao Wu^{1,2,3}  | Huan Jia^{1,2,3}

¹Department of Otolaryngology Head and Neck Surgery, Shanghai Ninth People's Hospital, Shanghai Jiao Tong University School of Medicine, Shanghai, China | ²Ear Institute, Shanghai Jiao Tong University School of Medicine, Shanghai, China | ³Shanghai Key Laboratory of Translational Medicine on Ear and Nose Diseases, Shanghai, China | ⁴Shanghai Jiao Tong University School of Medicine, Shanghai, China

Correspondence: Huan Jia (huan.jia.ori@shsmu.edu.cn)

Received: 8 January 2025 | **Accepted:** 9 March 2025

Funding: This work was supported by "National Double First-Class" and "Shanghai-Top-Level" high education initiative at Shanghai Jiao Tong University School of Medicine. HJ received the funding from Cross-disciplinary research fund of Shanghai Ninth People's Hospital (JYJC202209); Shanghai Talent Development Fund (2019047); Shanghai Key Laboratory of Translational Medicine on Ear and Nose Diseases (14DZ2260300). National Key Research and Development Program (2023YFB4705805).

Keywords: anatomic characteristics | external auditory canal | inner ear disease | round window

ABSTRACT

Objective: To clarify the feasibility and the anatomical characteristics related to round window exposure via the external auditory canal (EAC) without bony removal.

Methods: Surgical videos and radiological data from 50 adult patients who underwent endoscopic tympanoplasty type I were collected. According to surgical videos, round window niche (RWN) exposure was classified as "Certainly," "Possibly," and "None," and round window membrane (RWM) exposure was classified as "Clear visualization," "Incomplete visualization," "Just perceptible" and "Invisible." Basing on CT reconstruction, distances among RWM, RWN, tympanic annulus (TA), width, and orientation of scala tympani (ST) were measured under the Coordinate System of Cochlea, and anatomic features of EAC under the Coordinate System of EAC.

Results: 60% of RWNs were "Certainly," 24% "Possibly," and 16% "None" exposed. RWM exposure was 32% "Clear visualization," 22% "Incomplete visualization," 14% "Just perceptible," and 32% "Invisible." Longer distances between RWM and TA (RWM-TA), and the Width of ST in x and z sections were related to RWM exposure (RWM-TA: Spearman- $r=0.663$, $p<0.001$, ST in x: Spearman- $r=-0.337$, $p=0.017$, z: Spearman- $r=-0.586$, $p<0.001$). RWM-TA longer than 7.06 mm indicated a possibility of RWM exposure (AUC=0.784, $p=0.011$). Widths of ST in x and z sections shorter than 1.85 mm and 1.84 mm, respectively, indicated better RWM exposure (AUC=0.887, $p<0.001$). The size of EAC in axial and coronal sections could significantly predict RWM exposure (axial: AUC=0.726, $p=0.011$, coronal: AUC=0.798, $p=0.001$).

Conclusion: In adults, 54% of RWM could be partially visualized via EAC without bony removal. There are reliable pre-operative predictors for RWM exposure, which are helpful for future inner ear therapy.

Level of Evidence: 3

Jiayu Sun, Haoyue Tan, and Jianqing Chen have made equal contributions to this study.

This is an open access article under the terms of the [Creative Commons Attribution-NonCommercial-NoDerivs](https://creativecommons.org/licenses/by-nc-nd/4.0/) License, which permits use and distribution in any medium, provided the original work is properly cited, the use is non-commercial and no modifications or adaptations are made.

© 2025 The Author(s). *Laryngoscope Investigative Otolaryngology* published by Wiley Periodicals LLC on behalf of The Triological Society.

1 | Introduction

Inner ear pathology, characterized primarily by hearing loss, represents one of the most prevalent diseases worldwide [1, 2], and adversely affects the quality of life for millions of patients [3]. Pharmacological agents (PAs) are the primary method for treating these diseases. However, due to the blood-labyrinth barrier, systemic administration of PAs often fails to achieve effective concentrations within the inner ear [4]. Topical administration, by injecting through the tympanic membrane into the middle ear, has been extensively explored, with the expectation of PAs penetrating into the inner ear through the round window (RW) [5]. Nevertheless, recent studies demonstrated that drug efficacy largely depended on molecular diffusion across the RW membrane (RWM) [5–7]. The drainage of the eustachian tube is another challenging problem [8, 9].

Besides middle ear drug delivery system, direct administration of PA into inner ear via RWM has been performed in animal studies [10–12] and mostly via posterior tympanotomy approach in clinical practice [13, 14]. Although it facilitates drug dosage controlling, the posterior tympanotomy is still time-consuming, and the potential for traumatism to the inner ear cannot be ignored [15]. Hence, the procedure is always combined with inner ear opening such as cochlear implantation, and currently not a regular choice for clinical application.

With the advancements in endoscopy technology, a minimally invasive and time-saving approach for RWM micro-puncture through the external auditory canal (EAC) has emerged [16]. This might be more widely applied because of the initial success of inner ear gene therapy such as OTOF [17, 18]. Previous studies simply demonstrated the anatomic features and morphological variations of RW [19, 20]. They failed to find predictive factors of RWM exposure combining clinical and radiological data or considering the possibility of non-bony removal. Solving these problems would significantly promote the treatment of inner ear disease in a more practicable direction.

In this study, we intend to assess RW exposure by endoscopic view through EAC, and to construct a classification for clinical practice. The distance and angle among neighboring anatomical structures of RW were measured on computed tomography (CT) in order to find out reliable anatomical indicators of RW exposure difficulty and provide anatomical data for the designation of flexible robots and surgical tools via EAC.

2 | Methods

2.1 | Study Design

This retrospective study was approved by the Ethics Review Board (Ethical approval: SH9H-2023-T310-1) and complied with the amended Declaration of Helsinki. All the patients recruited have signed informed consent. Adult patients who underwent endoscopic tympanoplasty between January 2022 and June 2023 by two senior otologic surgeons were consecutively recruited. Inclusion criteria were: (1) Endoscopic tympanoplasty; (2) no bony erosion of the middle ear; (3)

no deformities in the external, middle, or inner ear; and (4) availability of surgical video and radiological numeric data. Patients were excluded if: (1) Intraoperative bony removal of the posterior wall of the EAC before assessing RW exposure; (2) RW was not clearly exposed due to blood or swollen mucosa; or (3) poor quality of either the surgical video or CT. Finally, medical data from 50 patients (27 females, 23 males, 48.2 ± 15.0 years), consisting of 25 left-side and 25 right-side cases, were included.

2.2 | Evaluation of RW Exposure From Surgical Video

Routinely, a 3 mm diameter, 15 cm length, 0° endoscope with a three-CCD camera system and a high-resolution monitor (Karl Storz, Tuttlingen, Germany) was used. A standardized surgical procedure of tympanoplasty was followed; the steps before RWN and RWM assessment were: elevating the tympanomeatal flap to reveal the tympanic cavity, identifying the RW location and ossicular chain without bony removal. Two otologic surgeons independently assessed the visibility of RWN and RWM. RWN exposure was categorized into three levels: “Certainly” exposed: where the anterior and posterior pillars, tegmen, and fustis [19] of RWN were all visible; “Possibly” exposed: where only portions of the pillars and tegmen were visible; “None” exposed: where only the tegmen was discernible or not at all. Referring to the St Thomas Hospital classification of RWM exposure via posterior tympanotomy [21], we classified RWM exposure into 4°. Degree 1 “Clear visualization”: more than 50% of RWM is visible; Degree 2 “Incomplete visualization”: 26%–50% of RWM is visible; Degree 3 “Just perceptible”: 1%–25% of RWM is visible; Degree 4 “Invisible”: RWM was not visible at all (Figure 1). To standardize the evaluation, we used the endoscopic image whose observing site was located around 3 mm lateral to the tympanic annulus (TA), closely adjacent to the posterior wall of the EAC.

2.3 | Measurements of Anatomical Features Around RW

Temporal bone CT images (0.625 mm slice thickness) of these patients were independently assessed by two otologic surgeons using the Horos DICOM viewer (Horos Project, Geneva, Switzerland) in a 3D MPR mode. The measured distances are denoted by uppercase letters, while angles are noted as “ \angle ” before letters.

Several measurements related to RWN, RWM, the orientation of modiolus axis, and the width of scala tympani (ST) under the Cochlear Coordinate System [22] were investigated (Table 1). In the axial view, (1) measurement related to RWN exposure included: “RWN-TA” denotes the distance from (the most prominent point of) RWN to (posterior edge of) TA. “RWM-PRO” measures the distance to which RWN protrudes from RWM plane. (2) Measurements related to RWM included: “RWM-TA” is the distance from (midpoint of) RWM to (posterior edge of) TA. “AW_EAC-RWM_TA” represents (perpendicular) distance from anterior wall of EAC to tangent line connecting (midpoint of) RWM and (posterior edge of) TA.

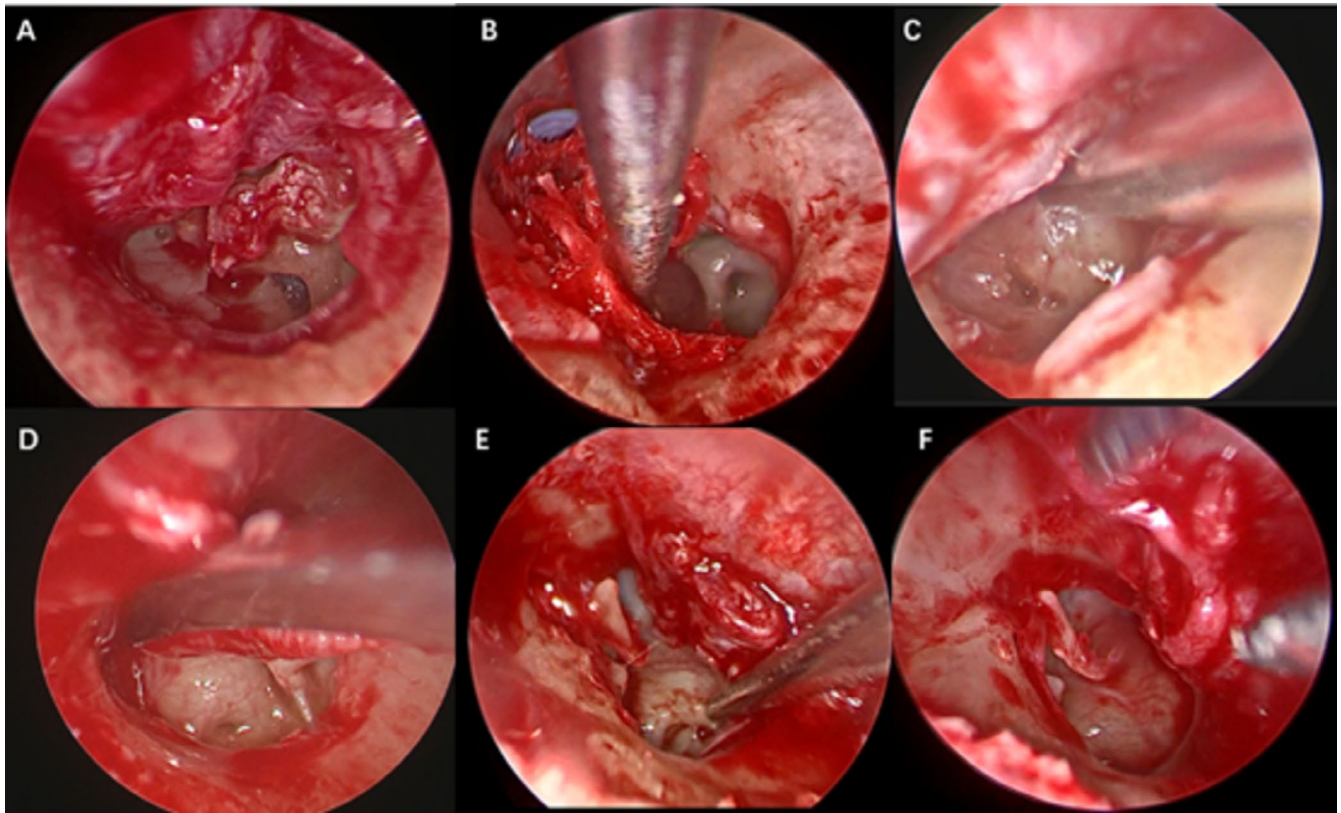


FIGURE 1 | Different exposures of Round Window Niche (RWN) and Membrane (RWM). (A, B) show “Clear visualization” of the RWM. (C) shows “Incomplete visualization.” (D) shows the RWM as “Just perceptible.” (E) shows the RWM as “Invisible” with “Possibly” exposure of the RWN. (F) shows the RWM as “Invisible” with the RWN “None” exposed.

“ \angle RWM-TA” describes the angle between the line connecting anterior to posterior margin of RWM and the line from (midpoint of) RWM to (posterior edge of) TA. (3) Measurements related to orientation of modiolus axis included: “ \angle basal_0-180-TA” is the angle formed by the line from the furthest end of basal turn to (posterior edge of) TA and the line from that end to (midpoint of) RWM. “ \angle basal_180-0-TA” is the angle between the line from (midpoint of) RWM to (posterior edge of) TA and the line from midpoint to the furthest end of basal turn. (4) Measurements related to width of ST: “WIDTH_ST_X” is the distance from (midpoint of) RWM to (lateral edge of) modiolus in x axis. The width of ST was also measured under z axis denoted as “WIDTH_ST_Z” [22].

The EAC Coordinate System was applied to measure the anatomic characteristics of the EAC and the operating pathway, with its axis aligned through the midpoint of the TA and the center of the bony EAC opening in both axial and coronal sections. “WIDTH_EAC” and “HEIGHT_EAC” represent the size of the bony EAC orifice in axial and coronal views, respectively. Similarly, “WIDTH_ISTHMUS” and “HEIGHT_ISTHMUS” denote the size of EAC isthmus, and “WIDTH_TA” and “HEIGHT_TA” indicate size of TA. “ \angle AW-TA-PW” is the angle formed by the line from the anterior bony EAC opening to (midpoint of) the TA and the line from the posterior bony EAC opening to (midpoint of) the TA in the axial section. “ \angle SW-TA-IW” is the angle between the line from the superior bony EAC opening to (midpoint of) the TA and the line from the inferior opening to (midpoint of) the TA in the coronal section (Table 2). These

measurements also provide insights into the potential range of endoscopic maneuverability.

2.4 | Visualization of RWM Exposure via EAC by 3D Modeling

To validate the reliability of subjective evaluation from surgical video, the degree of RWM exposure was further evaluated by 3D modeling. We utilized MIMICS 23.0 (Materialize, Leuven, Belgium) to segment and process the CT images. RWM area being observed at its best angle without any obstructing osseous structures was represented as RWM-3D-Ideal (Figure 2A). RWM area being observed through the posterior wall of EAC and factoring in a 1.5mm thickness simulating endoscope body obstruction (which was also the same as endoscope’s radius) was represented as RWM-3D-Reality (Figure 2B). The degree of RWM exposure was calculated as the ratio of RWM-3D-Reality/RWM-3D-Ideal, and was categorized similarly as outlined in Section 2.2.

2.5 | Statistical Analysis

Statistical analysis was conducted using SPSS version 25.0 (Chicago, IL, U.S.A.). A p -value <0.05 denoted statistical significance. Measurement data were expressed as Means \pm SD. Correlation between two evaluation ways of RWM exposure were analyzed using Kendall correlation analysis. Differences in measurements among exposure groups were assessed with one-way ANOVA. Correlations

TABLE 1 | Summary of the measurements in Cochlear Coordinate System.

Measurements	Description and clinical consideration	Example
RWN-TA	Distance between RWN and TA, also indicated the most superficial distance of needling	
RWM-PRO	Distance of RWN protruding from RWM in the axial section, also indicated the depth of RWN	
RWM-TA	Distance between RWM and TA, also indicated a proper depth of needling	
AW_EAC-RWM_TA	Distance of anterior wall of EAC to the tangent line of RWM to TA, also indicated the freedom of endoscope movement	
∠RWM-TA	Angle between the line drawn from anterior to posterior margin of RWM, and the line drawn from RWM to TA, might indicate the orientation of RWM	
∠basal_0-180-TA	Angle between the line drawn from the furthest end of the basal turn to TA, and the line drawn from that end to RWM, might indicate the orientation of basal turn and RWM	
∠basal_180-0-TA	Angle between the line drawn from RWM to TA, and the line drawn from RWM to the furthest end of basal turn, might indicate the orientation of basal turn and RWM	
WIDTH_ST_Z	Distance between RWM and modiolus in z axis, also indicated the width of ST, the orientation of RWM, and depth of RWM micro-puncture	
WIDTH_ST_X	Distance between RWM and modiolus in x axis also indicated the width of ST, the orientation of RWM, and depth of RWM micro-puncture	

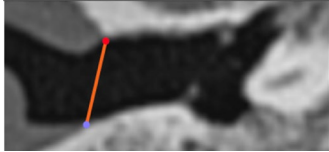
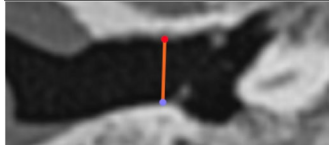
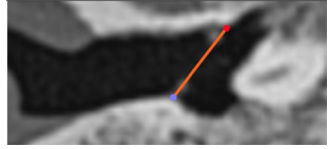
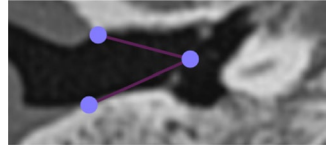
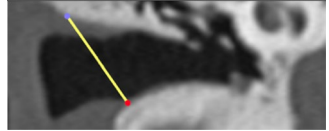
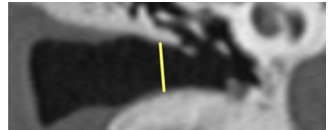
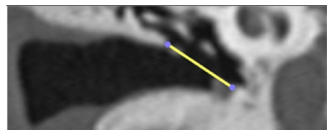
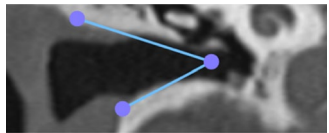
between measurements and exposure degrees were analyzed using Spearman's rank correlation and inter-class correlation coefficient. Receiver operating characteristic (ROC) curves were constructed to identify predictors for RWM and RWN exposure. Youden index, cut-off point, sensitivity, and specificity were achieved according to coordinate points of the ROC curve.

3 | Results

3.1 | Exposure of RWN and RWM

Based on surgical videos, 60% of RWNs were "Certainly" exposed, 24% "Possibly" and 16% "None" For RWM, "Clear

TABLE 2 | Summary of the measurements in the EAC Coordinate System.

Measurements	Description	Example
WIDTH_EAC	Width of bony EAC orifice in axial position	
WIDTH_ISTHMUS	Width of EAC isthmus in axial section	
WIDTH_TA	Width of TA in axial section, indicating the size of tympanic membrane	
\angle AW-TA-PW	Angle between the line from the anterior bony opening of EAC to TA, and the line from the posterior bony opening of EAC to TA in axial section	
HEIGHT_EAC	Width of bony EAC orifice in coronal section	
HEIGHT_ISTHMUS	Width of EAC isthmus in coronal section	
HEIGHT_TA	Width of TA in coronal section, indicating the size of tympanic membrane	
\angle SW-TA-IW	Angle between the line from superior wall of bony EAC to TA, and the line from inferior wall of bony EAC to TA in coronal section	

visualization” to “Invisible” was observed in 32%, 22%, 14%, and 32% of cases. Figure 3 illustrates RWM exposure percentages across different RWN categories. In instances with RWN “None” exposed, RWM was consistently obscured. As to RWN “Possibly” exposed, RWM was visible in 58.3% of the cases, and for “Certainly” exposed, 90% of the time. A significant correlation was noted between RWN and RWM exposures (Spearman $r=0.659$, $p<0.001$). In the 3D model, RWM Degrees 1 to 4 were 20%, 24%, 16%, and 40%, respectively. Notably, RWM exposure in surgical videos significantly correlated with those in the 3D model (Kendall tau_b $r=0.613$, $p<0.001$), verifying the reliability of classification from surgical video.

3.2 | Anatomical Features of Trans-Canal Approach for RWM Micro-Puncture and Anatomic Data for Clinical Practice

Table 3 and Figure S1 outline measurements pertinent to robotic manipulation and tool development. The robotic arm’s mobility ranges from 5.21 to 5.58 mm longitudinally with a 32.31°–34.95° of freedom, and 6.17–6.81 mm vertically with a 44.92°–49.86° of freedom. Under optimal conditions, an appropriate penetrating depth after passing TA is 7.07–7.62 mm. For a perpendicular (90°) micro-puncture into RWM, the needle should be pre-bent between 57.28° and 62.37°. Once the

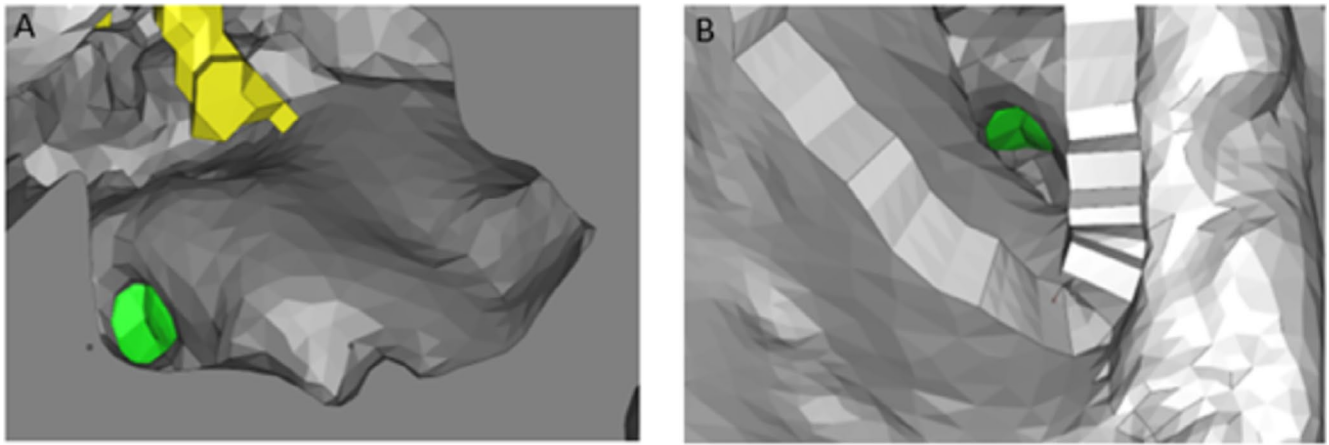


FIGURE 2 | Round window exposure on 3D modeling of External Auditory Canal (EAC). (A) shows an ideally view of the round window (green) from the EAC, and (B) shows a model of reality with a 1.5 mm thickness inside the bony EAC considering the otoscopic perspective and its radius. The ossicles were marked as yellow.

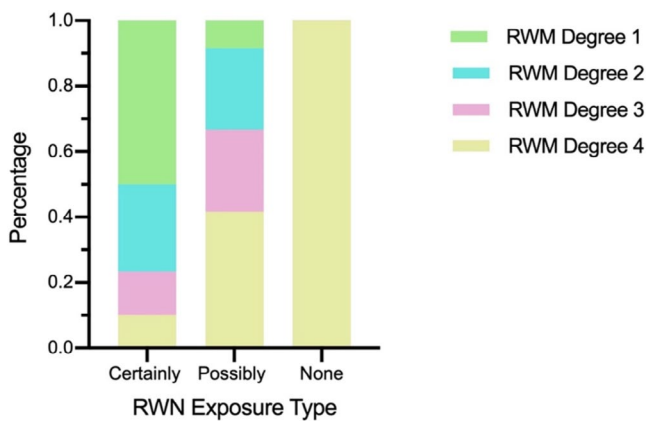


FIGURE 3 | Round window exposure and classification among 50 ears.

needle penetrates RWM, the recommended insertion depth is 1.71–1.87 mm to avoid harming themodiolus.

3.3 | Anatomic Characteristics Related to RWN and RWM Exposure

A longer distance of RWN-TA indicated a better RWN exposure with Spearman $r=0.483$, $p<0.001$. This distance was different among three RWN exposure groups ($F=7.224$, $p=0.002$). Post hoc analysis verified that it was significantly longer in the RWN “Certainly” exposed group compared with the other two.

A longer RWM-TA was related to a better RWM exposure (Spearman $r=0.663$, $p<0.001$). A shorter WIDTH_ST_Z and WIDTH_ST_X were correlated with a better RWM exposure (WIDTH_ST_Z: Spearman $r=0.586$, $p<0.001$, WIDTH_ST_X: Spearman $r=0.337$, $p=0.017$). The correlations were still significant when the orientation of cochlear (both \angle basal_180-0-TA and \angle basal_0-180-TA) was controlled (RWM-TA: partial correlation $r=0.647$, $p<0.001$ WIDTH_ST_Z: partial correlation $r=0.540$, $p<0.001$, WIDTH_ST_X: partial correlation $r=0.319$, $p=0.027$). WIDTH_ST_Z of “Invisible” group was significantly

larger than the other three ($F=9.073$, $p<0.001$). Results also showed that a wider WIDTH-EAC correlated with better RWM exposure (Spearman $r=0.428$, $p=0.002$). The orientation of cochlear, including \angle basal 0-180-TA and \angle basal 180-0-TA, and AW_EAC-RWM_TA were not related to RWM exposure.

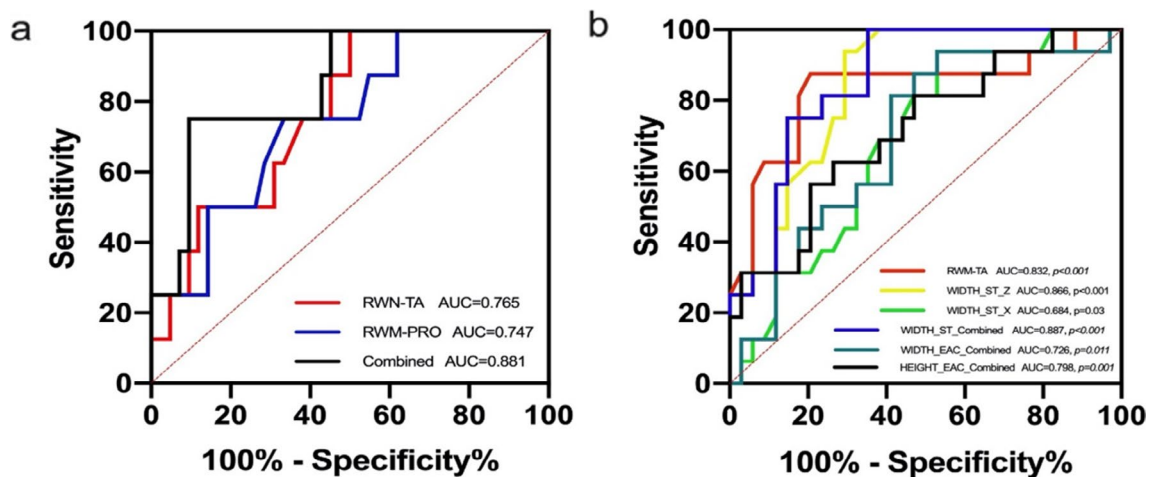
3.4 | Anatomic Characteristics Predicting Possibility of RWN and RWM Exposure

Based on Section 3.3 findings and requirements of clinical practice, we reclassified RWN exposure into two groups: “possible” (combining “Certainly” and “Possibly” exposed) and “impossible” (only “None” exposed). RWN-TA significantly predicted the possibility of RWN exposure with area under the curve (AUC)=0.765, $p=0.019$, sensitivity=50%, specificity=100%, Youden index=0.5, and cut-off point=5.79. RWM-PRO also predicted the possibility of RWN exposure with AUC=0.747, $p=0.028$; sensitivity=66.7%, specificity=75%, Youden index=0.417, and cut-off point=0.69. The combined predictive effect of the two factors was even larger with AUC=0.881, $p=0.001$, sensitivity=69%, specificity=100% (Figure 4A). This might be explained by a relatively distant view and protruding niche being conducive to providing a panorama of RWN.

Similarly, we reclassified RWM exposure into two groups: “Clear visualization,” “Incomplete visualization,” and “Just perceptible” as “possible” and “Invisible” as “impossible.” Factors related to RWM exposure were classified into three categories: RWM anatomic characteristics, width of ST, and EAC anatomic characteristics. According to ROC, RWM-TA significantly predicted the possibility of RWM exposure with AUC=0.832, $p<0.001$, sensitivity=79.4%, specificity=87.5%, Youden index=0.669, and cut-off point=7.06. Other measurements related to RWM anatomy failed to show significant predictive value. As to the width of ST, WIDTH_ST_Z and WIDTH_ST_X could also significantly predict the possibility of RWM exposure (WIDTH_ST_X: AUC=0.684, $p=0.038$, cut-off value=1.85; WIDTH_ST_Z: AUC=0.866, $p<0.001$, cut-off value=1.84), and their combined effect showed AUC (WIDTH_ST-combined)=0.887, $p<0.001$, sensitivity=86.7%,

TABLE 3 | Anatomical features of the surgical approach from EAC to RW in this classification.

	Clear visualization (95% CI)	Incomplete visualization (95% CI)	Just perceptible (95% CI)	Invisible (95% CI)	Average (95% CI)
DEPTH_EAC (mm)	12.6~14.1	11.2~13.5	12.0~13.9	12.5~14.0	11.2~14.0
WIDTH_EAC (mm)	7.88~8.94	7.64~9.19	7.50~9.09	7.53~8.55	7.99~8.54
HEIGHT_EAC (mm)	9.97~11.32	10.37~13.96	8.29~12.84	10.78~13.13	10.76~11.99
WIDTH_ISTHMUS (mm)	4.98~5.84	5.03~6.27	5.08~5.9	5.03~5.57	5.25~5.63
HEIGHT_ ISTHMUS (mm)	5.77~7.06	6.17~8.18	4.79~6.91	6.29~7.29	6.26~6.95
WIDTH_TA (mm)	8.63~9.24	8.67~9.60	8.47~9.04	8.36~9.20	8.71~9.08
HEIGHT_TA (mm)	8.93~9.67	8.31~9.68	8.10~10.16	8.52~9.22	8.84~9.30
∠AW-TA-PW(°)	31.24~36.6	29.93~35.72	28.79~39.64	30.55~35.44	32.09~34.79
∠SW-TA-IW(°)	42.25~49.08	39.18~55.32	40.05~49.24	43.61~54.94	44.51~49.54
RWM-TA	7.40~8.10	7.30~7.87	6.41~7.03	6.37~7.04	7.03~7.45
∠RWM-TA (°)	26.35~32.95	23.65~37.39	18.06~36.42	23.14~36.04	26.71~32.15
∠EAC-TYM-RW_X (°)	129~142	121~137	117~135	117~139	117~140
∠EAC-TYM-RW_Z (°)	111~164	113~158	128~157	114~142	120~158
RWN-PRO(mm)	0.65~0.80	0.64~0.83	0.57~0.98	0.62~0.76	0.61~0.95
∠basal_0-180-TA (°)	12.95~15.78	14.35~16.55	12.36~15.98	13.16~16.15	13.93~15.33
∠basal_180-0-TA (°)	144.23~148.95	144.96~148.98	141.19~150.12	142.52~146.95	144.98~147.32
WIDTH_ST_X (mm)	1.72~2.07	1.78~2.30	1.78~2.34	2.01~2.31	1.94~2.13
WIDTH_ST_Z (mm)	1.52~1.74	1.63~2.00	1.78~2.33	1.96~2.29	1.74~1.94

**FIGURE 4** | Sensitivity and specificity of the predictive value of anatomical landmarks related to RWN (A) and RWM (B) exposure.

specificity=80%, Youden index=0.665. Considering EAC anatomic characteristics, only combined factors of axial (WIDTH_EAC, WIDTH_ISTHMUS, WIDTH_TA, and ∠AW-TA-PW) and coronal (HEIGHT_EAC, HEIGHT_ISTHMUS, HEIGHT_TA, and ∠SW-TA-IW) respectively showed significant predictive

effects: AUC (WIDTH-combined)=0.726, $p=0.011$, sensitivity=93.3%, specificity=60%, Youden index=0.533; AUC (HEIGHT-combined)=0.798, $p=0.001$, sensitivity=66.7%, specificity=86.7%, Youden index=0.534. More details were shown in Table 4 and Figure 4B.

TABLE 4 | Predictive value of the anatomical landmarks related to RWM exposure.

	AUC	<i>p</i>	Sensitivity	Specificity	Youden index	Cut-off
RWM-TA(mm)	0.832	<0.001*	79.4%	87.5%	0.669	7.06
WIDTH_ST_X(mm)	0.684	0.038*	93.8%	47.1%	0.409	1.85
WIDTH_ST_Z(mm)	0.866	<0.001*	93.8%	73.5%	0.673	1.84
WIDTH_ST(combined)	0.887	<0.001*	86.7%	80%	0.665	N/A
WIDTH_EAC-combined	0.726	0.011*	93.3%	60%	0.533	N/A
HEIGHT_EAC-combined	0.798	0.001*	66.7%	86.7%	0.534	N/A

**p* < 0.05.

4 | Discussion

Within our knowledge, our study is the first to provide a classification of RWM exposure via EAC under a natural approach without bony removal. We also provide predictive landmarks of RWM exposure based on human clinical data and present a quick and simple 3D modeling method for easy visualization. We found the width of the ST, the distance between the RWM and TA, and the size of the EAC were reliable predictors of RWM exposure. Our findings could significantly contribute to the innovative management of inner ear diseases, such as gene therapy and perilymph sampling. They can aid in estimating surgical difficulty and guide the preparation for micro-drilling. Furthermore, our research can facilitate the development of specialized tools or robotic systems to enhance the safety and effectiveness of these surgical procedures.

4.1 | Classification of RWM Exposure for EAC Approach

Except for a few articles [19, 23, 24], previous studies have primarily concentrated on RWM exposure via posterior tympanotomy. While this approach generally allows for adequate RW exposure [25], studies have identified specific factors—particularly the facial nerve and its anatomical relationship with surrounding structures—hampering RWM exposure [26, 27]. In contrast, our study focused on RWM exposure via EAC without bony drilling, which is more suitable for the current trend of minimal invasive management [28, 29]. Based on clinical feedback, not all patients' RWM can be fully exposed [30]. Aslan et al. [31] concluded a 75% probability of RWN exposure, and the probability of RWM was even less via EAC. Thus, a new classification of RWM exposure via EAC should be established.

Traditional St. Thomas Hospital classification was based on posterior tympanotomy approach [21], as type I for 100% exposure, type IIa for more than 50%, type IIb for less than 50%, and type III for 0%. With this definition, the RWM exposure via EAC in our study might be unbalanced as type I 2%, type IIa 30%, type IIb 36%, type III 32%. Considering the main purpose of this study is to assess the possibility of a natural approach for RWM micro-puncture, we introduced a novel classification. Our findings revealed that only 32% of RWM could be sufficiently exposed, and 54% could be exposed, and this ratio

was coordinated with 3D modeling. The rationale for our classification is based on clinical practice, as Degree 1 indicates a convenient and direct RWM micro-puncture, while Degree 2 indicates a tortuous pathway for micro-puncture but could still be possible under certain positions and customized surgical instruments. It is rather hard to puncture RWM in Degree 3 so that a robotic manipulation and appropriate bone drilling should be considered. As to Degree 4, the posterior wall of EAC should be drilled or RWM micro-puncture via EAC should be discarded.

4.2 | Classifying by 0° or Angled Endoscope

It seems that an angled endoscope, for example, 30°, would provide a better view of tilt structures such as RW. However, the angled endoscope needs to be inserted deeper or additionally bent at a certain angle after passing TA in order to vertically observe RWM [23, 24, 29]. We found that enough space in the vertical direction is very important for an angled view. In the situation where RW could be exposed, an angled endoscope may facilitate exposure. However, if RW is hard to expose, deeper insertion may only elevate the risk of inner ear injury. This may also explain why most of the stapes surgeries were performed under a 0° endoscope [32]. Therefore, we believe that classification by a 0° endoscope provides more practical value.

4.3 | Predictors of RWM Exposure Under Endoscope via EAC

Anatomic features that might influence RWM exposure were measured both on the Cochlear Coordinate System and the EAC Coordinate System in order to obtain an easy and standard protocol for prediction. Results showed that a relatively narrower ST (anterior-medial orientated RWM) and a larger EAC favor RWM exposure. Longer distances from RWM to TA also effectively predict better RWM exposure, likely because a more distant perspective offers a comprehensive view of RWM. To our knowledge, our study is the first proposing these indicators from real clinical practice data instead of animal studies or cadaveric temporal bones. As these measurements are easily assessed during clinical practice, we believe our study may greatly assist in making clinical decisions for the trans-canal RW approach to inner ear therapy.

4.4 | Clinical Data Support for the Designation of Surgical Tools or Robots for Micro-Manipulation on RWM via EAC

PAs through RWM from EAC is emerging as the primary treatment approach for inner ear diseases. Utilizing the natural body lumen, endoscopic manipulation reduces the need for extensive bone drilling, minimizes internal ear damage, and shortens surgical time. The use of long, thin instruments with sub-millimetric precision and precise amplitude of motion is crucial for both manual and robotic manipulation.

A significant advancement in this area is the development of syringes for RWM micro-puncture [14]. However, there is still a lack of reference data for microneedles, particularly for micro-puncture from the EAC. Fujita et al. [24] analyzed axial CT slices of cadaveric temporal bone, revealing several anatomic data of RW. We achieved a similar results and further expanded the parameter database. These data were conducive to designating the pre-bent angle of the needle and were valuable in determining the angle and depth of needle insertion.

4.5 | Limitation

Manual measurements are prone to errors. Future evaluations could benefit from the precision of artificial intelligence and machine learning. Furthermore, a larger sample size is essential to confirm our study's findings.

5 | Conclusion

For most adults, RWM could be at least partially exposed via EAC. The distance between RWM and TA, the width of ST, and the size of EAC were reliable predictors of the possibility of RWM exposure and even micro-puncture. Our result provided an operational basis for inner ear gene therapy. The data we achieved also facilitate the designation of syringes, tools, or robots for the micro-manipulation of RW via EAC.

Acknowledgments

We are in sincere and deep gratitude to the participants for their participation in this study. We would like to express our gratitude to Yuqi Jiang for his selfless and timely assistance in this study.

Conflicts of Interest

The authors declare no conflicts of interest.

References

1. D. Baguley, D. McFerran, and D. Hall, "Tinnitus," *Lancet (London, England)* 382, no. 9904 (2013): 1600–1607, [https://doi.org/10.1016/S0140-6736\(13\)60142-7](https://doi.org/10.1016/S0140-6736(13)60142-7).
2. C. M. Jarach, A. Lugo, M. Scala, et al., "Global Prevalence and Incidence of Tinnitus: A Systematic Review and Meta-Analysis," *JAMA Neurology* 79, no. 9 (2022): 888, <https://doi.org/10.1001/jamaneurol.2022.2189>.

3. M. C. Holley, "Keynote Review: The Auditory System, Hearing Loss and Potential Targets for Drug Development," *Drug Discovery Today* 10, no. 19 (2005): 1269–1282, [https://doi.org/10.1016/S1359-6446\(05\)03595-6](https://doi.org/10.1016/S1359-6446(05)03595-6).
4. A. A. McCall, E. E. Swan, J. T. Borenstein, W. F. Sewell, S. G. Kujawa, and M. J. McKenna, "Drug Delivery for Treatment of Inner Ear Disease: Current State of Knowledge," *Ear and Hearing* 31, no. 2 (2010): 156–165, <https://doi.org/10.1097/AUD.0b013e3181c351f2>.
5. G. Licameli, P. Johnston, J. Luz, J. Daley, and M. Kenna, "Phosphorylcholine-Coated Antibiotic Tympanostomy Tubes: Are Post-Tube Placement Complications Reduced?," *International Journal of Pediatric Otorhinolaryngology* 72, no. 9 (2008): 1323–1328, <https://doi.org/10.1016/j.ijporl.2008.05.018>.
6. M. V. Goycoolea, "Clinical Aspects of Round Window Membrane Permeability Under Normal and Pathological Conditions," *Acta Otolaryngologica* 121, no. 4 (2001): 437–447, <https://doi.org/10.1080/000164801300366552>.
7. N. El Kechai, F. Agnely, E. Mamelle, Y. Nguyen, E. Ferrary, and A. Bochet, "Recent Advances in Local Drug Delivery to the Inner Ear," *International Journal of Pharmaceutics* 494, no. 1 (2015): 83–101, <https://doi.org/10.1016/j.ijpharm.2015.08.015>.
8. S. K. Plontke, A. A. Mikulec, and A. N. Salt, "Rapid Clearance of Methylprednisolone After Intratympanic Application in Humans. Bird PA, Begg EJ, Zhang M, et al. Intratympanic Versus Intravenous Delivery of Methylprednisolone to Cochlear Perilymph. Otol Neurotol 2007;28:1124–30," *Otology & Neurotology: Official Publication of the American Otological Society, American Neurotology Society [and] European Academy of Otology and Neurotology* 29, no. 5 (2008): 732–733, <https://doi.org/10.1097/MAO.0b013e318173fcea>.
9. M. E. Hoffer, K. Allen, R. D. Kopke, P. Weisskopf, K. Gottshall, and D. Wester, "Transtympanic Versus Sustained-Release Administration of Gentamicin: Kinetics, Morphology, and Function," *Laryngoscope* 111, no. 8 (2001): 1343–1357, <https://doi.org/10.1097/00005537-200108000-00007>.
10. A. N. Salt, D. B. Sirjani, J. J. Hartsock, R. M. Gill, and S. K. Plontke, "Marker Retention in the Cochlea Following Injections Through the Round Window Membrane," *Hearing Research* 232, no. 1–2 (2007): 78–86, <https://doi.org/10.1016/j.heares.2007.06.010>.
11. H. Hahn, A. N. Salt, T. Biegner, et al., "Dexamethasone Levels and Base-To-Apex Concentration Gradients in the Scala Tympani Perilymph After Intracochlear Delivery in the Guinea Pig," *Otology & Neurotology* 33, no. 4 (2012): 660–665, <https://doi.org/10.1097/MAO.0b013e318254501b>.
12. C. M. Kelso, H. Watanabe, J. M. Wazen, et al., "Microperforations Significantly Enhance Diffusion Across Round Window Membrane," *Otology & Neurotology* 36, no. 4 (2015): 694–700, <https://doi.org/10.1097/MAO.0000000000000629>.
13. S. Leong, A. Aksit, S. J. Feng, J. W. Kysar, and A. K. Lalwani, "Inner Ear Diagnostics and Drug Delivery via Microneedles," *Journal of Clinical Medicine* 11, no. 18 (2022): 5474, <https://doi.org/10.3390/jcm11185474>.
14. H. Chiang, M. Yu, A. Aksit, et al., "3D-Printed Microneedles Create Precise Perforations in Human Round Window Membrane In Situ," *Otology & Neurotology* 41, no. 2 (2020): 277–284, <https://doi.org/10.1097/MAO.0000000000002480>.
15. J. Je'menica and A. Bajec-Opařina, "Sudden Hearing Loss in Children," *Clinical Pediatrics* 53, no. 9 (2014): 874–878.
16. P. Canzi, I. Avato, M. Manfrin, et al., "Anatomic Variations of the Round Window Niche: Radiological Study and Related Endoscopic Anatomy," *Surgical and Radiologic Anatomy* 41, no. 7 (2019): 853–857, <https://doi.org/10.1007/s00276-019-02225-8>.
17. M. Nieratschker, E. Yildiz, J. Schnoell, et al., "Intratympanic Substance Distribution After Injection of Liquid and Thermosensitive Drug

- Carriers: An Endoscopic Study,” *Otology & Neurotology: Official Publication of the American Otological Society, American Neurotology Society [and] European Academy of Otology and Neurotology* 43, no. 10 (2022): 1264–1271, <https://doi.org/10.1097/MAO.0000000000003729>.
18. J. Lv, H. Wang, X. Cheng, et al., “AAV1-hOTOF Gene Therapy for Autosomal Recessive Deafness 9: A Single-Arm Trial,” *Lancet* 403, no. 10441 (2024): 2317–2325, [https://doi.org/10.1016/S0140-6736\(23\)02874-X](https://doi.org/10.1016/S0140-6736(23)02874-X).
19. D. Marchioni, D. Soloperto, E. Colleselli, M. F. Tatti, N. Patel, and N. Jufas, “Round Window Chamber and Fustis: Endoscopic Anatomy and Surgical Implications,” *Surgical and Radiologic Anatomy* 38, no. 9 (2016): 1013–1019, <https://doi.org/10.1007/s00276-016-1662-5>.
20. D. Marchioni, M. Alicandri-Ciufelli, D. D. Pothier, A. Rubini, and L. Presutti, “The Round Window Region and Contiguous Areas: Endoscopic Anatomy and Surgical Implications,” *European Archives of Oto-Rhino-Laryngology* 272, no. 5 (2015): 1103–1112, <https://doi.org/10.1007/s00405-014-2923-8>.
21. A. C. Leong, D. Jiang, A. Agger, and A. Fitzgerald-O’Connor, “Evaluation of Round Window Accessibility to Cochlear Implant Insertion,” *European Archives of Oto-Rhino-Laryngology* 270, no. 4 (2013): 1237–1242, <https://doi.org/10.1007/s00405-012-2106-4>.
22. B. M. Verbist, M. W. Skinner, L. T. Cohen, et al., “Consensus Panel on a Cochlear Coordinate System Applicable in Histologic, Physiologic, and Radiologic Studies of the Human Cochlea,” *Otology & Neurotology: Official Publication of the American Otological Society, American Neurotology Society [and] European Academy of Otology and Neurotology* 31, no. 5 (2010): 722–730, <https://doi.org/10.1097/MAO.0b013e3181d279e0>.
23. A. Jain, R. Sharma, J. C. Passey, R. Meher, and R. Bansal, “Endoscopic Visualisation of the Round Window During Cochlear Implantation,” *Journal of Laryngology and Otology* 134, no. 3 (2020): 219–221, <https://doi.org/10.1017/S0022215120000067>.
24. T. Fujita, J. E. Shin, M. Cunnane, et al., “Surgical Anatomy of the Human Round Window Region: Implication for Cochlear Endoscopy Through the External Auditory Canal,” *Otology & Neurotology* 37, no. 8 (2016): 1189–1194, <https://doi.org/10.1097/MAO.0000000000001074>.
25. S. Jain, P. T. Deshmukh, P. Lakhota, S. Kalambe, D. Chandravanshi, and M. Khatri, “Anatomical Study of the Facial Recess With Implications in Round Window Visibility for Cochlear Implantation: Personal Observations and Review of the Literature,” *International Archives of Otorhinolaryngology* Jul 2019;23(3):e281–e291. 23, no. 3 (2019): e281–e291, <https://doi.org/10.1055/s-0038-1676100>.
26. L. H. Xie, J. Tang, W. J. Miao, X. L. Tang, H. Li, and A. Z. Tang, “Preoperative Evaluation of Cochlear Implantation Through the Round Window Membrane in the Facial Recess Using High-Resolution Computed Tomography,” *Surgical and Radiologic Anatomy* 40, no. 6 (2018): 705–711, <https://doi.org/10.1007/s00276-018-1972-x>.
27. S. Elzayat, I. Soltan, M. Talaat, and Y. A. Fouad, “The Role of High-Resolution Computer Tomography in Prediction of the Round Window Membrane Visibility and the Feasibility of the Round Window Electrode Insertion,” *European Archives of Oto-Rhino-Laryngology* 278, no. 9 (2021): 3283–3290, <https://doi.org/10.1007/s00405-020-06417-6>.
28. S. K. Plontke, P. K. Plinkert, B. Plinkert, A. Koitschev, H. P. Zenner, and H. Lowenheim, “Transtympanic Endoscopy for Drug Delivery to the Inner Ear Using a New Microendoscope,” *Advances in Oto-Rhino-Laryngology* 59 (2002): 149–155, <https://doi.org/10.1159/000059253>.
29. L. Migirov, Y. Shapira, and M. Wolf, “The Feasibility of Endoscopic Transcanal Approach for Insertion of Various Cochlear Electrodes: A Pilot Study,” *European Archives of Oto-Rhino-Laryngology* 272, no. 7 (2015): 1637–1641, <https://doi.org/10.1007/s00405-014-2995-5>.
30. D. Marchioni, A. Grammatica, M. Alicandri-Ciufelli, E. Genovese, and L. Presutti, “Endoscopic Cochlear Implant Procedure,” *European Archives of Oto-Rhino-Laryngology* 271, no. 5 (2014): 959–966, <https://doi.org/10.1007/s00405-013-2490-4>.
31. A. A. GnK, G. Eskiizmir, and A. Elhan, “Anatomic Observations on Variations of the Round Window Niche and Its Relationship to the Tympanic Membrane,” *Journal of International Advanced Otology* 2 (2006): 52–57.
32. R. Bartel, J. J. Sanz, I. Clemente, et al., “Endoscopic Stapes Surgery Outcomes and Complication Rates: A Systematic Review,” *European Archives of Oto-Rhino-Laryngology* 278, no. 8 (2021): 2673–2679, <https://doi.org/10.1007/s00405-020-06388-8>.

Supporting Information

Additional supporting information can be found online in the Supporting Information section.